NASA/TM—2014–217500

Laser Ablation Cleaning of Self-Reacting Friction Stir Weld Seam Surfaces: A Preliminary Evaluation

A.C. Nunes, Jr., C.K. Russell, and S.A. Brooke
Marshall Space Flight Center, Huntsville, Alabama

Q. Parry
University of Utah, Salt Lake City, Utah

N.M. Lowrey
Jacobs ESSSA Group, Huntsville, Alabama

February 2014

The NASA STI Program…in Profile

Since its founding, NASA has been dedicated to the advancement of aeronautics and space science. The NASA Scientific and Technical Information (STI) Program Office plays a key part in helping NASA maintain this important role.

The NASA STI Program Office is operated by Langley Research Center, the lead center for NASA's scientific and technical information. The NASA STI Program Office provides access to the NASA STI Database, the largest collection of aeronautical and space science STI in the world. The Program Office is also NASA's institutional mechanism for disseminating the results of its research and development activities. These results are published by NASA in the NASA STI Report Series, which includes the following report types:

- TECHNICAL PUBLICATION. Reports of completed research or a major significant phase of research that present the results of NASA programs and include extensive data or theoretical analysis. Includes compilations of significant scientific and technical data and information deemed to be of continuing reference value. NASA's counterpart of peer-reviewed formal professional papers but has less stringent limitations on manuscript length and extent of graphic presentations.

- TECHNICAL MEMORANDUM. Scientific and technical findings that are preliminary or of specialized interest, e.g., quick release reports, working papers, and bibliographies that contain minimal annotation. Does not contain extensive analysis.

- CONTRACTOR REPORT. Scientific and technical findings by NASA-sponsored contractors and grantees.

- CONFERENCE PUBLICATION. Collected papers from scientific and technical conferences, symposia, seminars, or other meetings sponsored or cosponsored by NASA.

- SPECIAL PUBLICATION. Scientific, technical, or historical information from NASA programs, projects, and mission, often concerned with subjects having substantial public interest.

- TECHNICAL TRANSLATION. English-language translations of foreign scientific and technical material pertinent to NASA's mission.

Specialized services that complement the STI Program Office's diverse offerings include creating custom thesauri, building customized databases, organizing and publishing research results…even providing videos.

For more information about the NASA STI Program Office, see the following:

- Access the NASA STI program home page at <http://www.sti.nasa.gov>

- E-mail your question via the Internet to <help@sti.nasa.gov>

- Phone the NASA STI Help Desk at 757–864–9658

- Write to:
  NASA STI Information Desk
  Mail Stop 148
  NASA Langley Research Center
  Hampton, VA 23681–2199, USA

NASA/TM—2014–217500

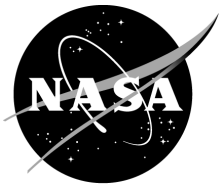

Laser Ablation Cleaning of Self-Reacting Friction Stir Weld Seam Surfaces: A Preliminary Evaluation

A.C. Nunes, Jr., C.K. Russell, and S.A. Brooke
Marshall Space Flight Center, Huntsville, Alabama

Q. Parry
University of Utah, Salt Lake City, Utah

N.M. Lowrey
Jacobs ESSSA Group, Huntsville, Alabama

National Aeronautics and
Space Administration

Marshall Space Flight Center • Huntsville, Alabama 35812

February 2014

Acknowledgments

The authors gratefully acknowledge the contributions of the laser cleaning system participants: Nathan Jonjevic of Adapt Laser Systems, LLC, Kansas City, MO; Robert Cargill of General Lasertronics Corp., San Jose, CA; and Matt Cash of the Marshall Space Flight Center Structural Strength Test Branch, for cleaning, packaging, and delivery of the test panels for this study.

TRADEMARKS

Available from:

NASA STI Information Desk
Mail Stop 148
NASA Langley Research Center
Hampton, VA 23681–2199, USA
757–864–9658

This report is also available in electronic form at
<http://www.sti.nasa.gov>

TABLE OF CONTENTS

LIST OF FIGURES

LIST OF FIGURES (Continued)

LIST OF TABLES

LIST OF ACRONYMS AND SYMBOLS

C-FSW	conventional friction stir welding
EDS	energy dispersive x-ray spectroscopy
FSW	friction stir welding
HAZ	heat-affected zone (of a weld)
MSFC	Marshall Space Flight Center
Nd:YAG	yttrium aluminum garnet ($Y_3Al_5O_{12}$) doped with a small amount of neodymium (a laser medium)
ROD	residual oxide defect
SEM	scanning electron microscopy
SR-FSW	self-reacting friction stir welding

NOMENCLATURE

c	diameter of (penny-shaped) crack
E	elastic modulus
L	length
r	radius
μ	surface energy
σ	tensile stress
σ_{fracture}	tensile fracture stress
τ	shear stress

TECHNICAL MEMORANDUM

LASER ABLATION CLEANING OF SELF-REACTING FRICTION STIR WELD SEAM SURFACES: A PRELIMINARY EVALUATION

1. INTRODUCTION

This Technical Memorandum is based upon a student research project carried out by the Metals Joining and Processes Branch of the Materials and Processes Laboratory of Marshall Space Flight Center (MSFC) during the summer of 2012 by Q. Parry, a junior in the Materials Science and Engineering Department at the University of Utah. C.K. Russell, S.A. Brooke, and N.M. Lowrey assisted the study entitled, "An Evaluation of Current Laser Ablation Technologies for Weld Surface Cleaning for Self-Reacting Friction Stir Welding."

Oxides and any solid contaminants residing on a weld seam and not destroyed by the friction stir welding (FSW) process are embedded in the trace of the seam within the weld 'nugget,' where they disturb subsequent deformation processes and may reduce the strength of the weld substantially. This condition is called residual oxide defect (ROD). Although the FSW process is not regarded as especially sensitive to seam surface contamination, heavy surface contamination can reduce weld strength substantially. Hence, seam surfaces to be welded by the FSW process are customarily manually cleaned during weld preparation.

Conventional manual cleaning processes dissolve and flush away greasy contaminants and abrade or scrape away insoluble contaminants and surface oxides. Lasers can deliver a power pulse to contaminants that can break them up through transient thermal stresses and explode them off with sudden vaporization. This study was undertaken to see if laser cleaning of weld seam surfaces prior to FSW could clean as well or better than conventional manual processes and might be a candidate for mechanization of the cleaning process.

1.1 Laser Terminology

As the name (an acronym for 'light amplification by stimulated emission of radiation') implies, lasers produce intense beams of light by stimulating excited electrons in a 'gain medium' to emit additional light that adds (in phase) to and intensifies the stimulating light beam. In the present case, the gain medium is Nd:YAG, i.e., yttrium aluminum garnet ($Y_3Al_5O_{12}$) doped with a small amount of neodymium. Ionized neodymium centers (Nd^{3+}) bind electrons (the bonding energy is reduced by the surrounding medium), and energy level gap transitions produce light in the infrared range. Nd:YAG lasers generally operate at a wavelength of 1,064 nm, although other energy level gaps (940, 1,120, 1,320, 1,440 nm) exist. The electrons are 'pumped' to higher energy levels by a flash lamp or laser diode light source.

The amplified beam is passed back and forth through the gain medium by bounding mirrors. Conceived as an oscillator, the laser is assigned a 'Q' factor, defined as the energy stored in the oscillation divided by the energy loss per cycle. Strong reflectors at boundaries retain oscillations within the lasing medium with little loss and the Q factor is high. A partial transmission through one mirror results in emission of a continuous wave laser beam. When one mirror is suddenly switched off, with a fully pumped beam an extremely high-energy pulse of light leaves the laser; under this high power loss condition, the lasing medium has a low Q factor. Switching the mirror on and off is called 'Q-switching.' In the present study, three Q-switched Nd:YAG lasers producing a succession of high power pulses of infrared light were used: a 300 W laser at Adapt Laser Systems in Kansas City, MO; a 240 W laser at General Lasertronics Corporation in San Jose, CA; and a 20 W Adapt Laser System at MSFC.

1.2 Laser Cleaning

The free electrons circulating in metallic bodies reflect electromagnetic radiation strongly at visible and infrared frequencies; metals are not greatly affected by visible and infrared light unless it is very intense, say on the order of 10^3 W/mm^2. For power densities having this or greater magnitude melting and evaporation occur at the metal surface, a vapor cavity forms, and the laser welding process begins.

Electric charge in insulators is relatively tightly bound together so that the forces exerted by the oscillating electromagnetic field of a light beam excites strong oscillations of heavy ions and produces large heating effects. Because of this difference in power absorption, and because most surface contaminants are nonmetallic, infrared radiation is a good candidate for removing surface contaminants. But the power must be delivered rapidly, so that it is carried away in contaminant vapor and particulates and does not merely heat the contaminants and allow appreciable heat conduction to the metal substrate.

1.3 Friction Stir Welding

FSW is a solid-state process in which a rotating pin is inserted into the weld seam and translated along the seam. A plug of metal sticks to and rotates with the pin. The shearing metal separating the rotating plug and stationary weld panel is concentrated within a narrow 'adiabatic shear band,' effectively a shear surface.

The seam enters the rotating plug as the shear surface advances. The segment of seam straddling the shear surface moves faster inside the rotating plug than outside in the stationary weld metal. Hence, the seam is stretched out, and a great deal of fresh, uncontaminated metal surface is exposed within the seam. The acting pressure forces the clean metal into complete contact and under the circumstances, the metallic bond extends across the seam so that the metal is welded. The stretched seam is recompressed as the rotating plug abandons it, but the seam remains welded; however, oxides and dirt from the original seam surface are embedded in the metal along the trace of the seam.

Accompanying the rapid, concentrated shearing at the shear surface is a relatively slow (creeping?) distributed shear process, which typically takes the form of a ring vortex or ring vortices surrounding the pin as shoulder scrolls and/or pin threads drive the flow radially inwards along the shoulder and axially down the pin, respectively. Two distinct kinds of FSW process are in common use: (1) The conventional friction stir welding (C-FSW) process, where the pin and shoulder press into the workpiece against a stationary anvil, and (2) the self-reacting friction stir welding (SR-FSW) process, where two shoulders rotating with the tool squeeze the workpiece and confine the weld metal at the tool.

The radial inflow at the shoulder(s) holds the seam on the rotating plug longer, where it is shifted toward the advancing side of the tool as it emerges. The radial outflow toward the anvil (C-FSW) or at the center of the pin (SR-FSW) expels the seam earlier from the rotating plug, where it is shifted toward the retreating side of the tool. Hence, in the longitudinal section, the seam trace is no longer a straight line parallel to the axis of the tool, but a curve, which may be easy to see in section, particularly if it is decorated with surface oxide particles. The series of curves seen in longitudinal section becomes the 'onion ring' pattern seen in transverse section.

1.4 The Effect of Contamination on Weld Strength

Weld tensile test coupons tend to deform by shear on 45º planes, where the shear stress is at a maximum. But not all 45º planes exhibit slip. Slip is limited to the softest, easiest slipping planes. As the planes work harden and match harder neighboring planes, the slip zone broadens. As slip deformation continues, the surface contours of the coupon indent. If nothing interrupts this process, it proceeds until the cross section of the coupon reduces to zero.

Long before this happens, the load supported by the coupon reaches its maximum when the work hardening rate is no longer able to keep up with the rate of area reduction. In a constant load (flexible) testing machine, the coupon fractures at this point of plastic instability, i.e., at the maximum load. In a constant deformation rate (stiff) testing machine, the load is allowed to decline and the coupon fractures at zero load and zero area. In a real testing machine, a perfectly ductile test coupon would fracture somewhere between these two extremes. The fracture surface would, however, neck down to zero.

Normally, the deformation process is interrupted before the coupon can neck to the zero area. Real metals are full of defects. Aside from linear dislocation defects responsible for work hardening, metals contain a distribution of microvoids. Over a slip plane, microvoids expand and coalesce, reducing the area in a kind of internal necking process, which becomes unstable and leads to fracture along a slip plane. The residues of the distorted microvoids can be seen on the fracture surface as 'shear dimples.'

In hot (high tool rpm and low weld speed) friction stir welds, the heat-affected zone (HAZ) tends to soften and broaden while the mechanically deformed nugget regions tend to retain higher strength. Such welds tend to exhibit necking located in the HAZ and 45º fracture surfaces.

Defects large enough to stand out above microvoids can cause larger internal instabilities and reduce strength still further. The classic model for larger defects is the Griffith theory of crack-induced brittle fracture modified by E. Orowan to apply to a ductile metal. In this model a penny-shaped crack of diameter c is taken to release elastic energy $\sigma^2 / 2E\left[4/3\pi(c/2)^3\right]$ contained in the sphere circumscribing the crack, where the stress is σ, and the elastic modulus is E. If the released elastic energy increment is enough to supply the new surface energy $\mu[2(\pi cdc)]$, where μ is the surface energy, then it is assumed that the crack propagates unstably through the medium. The stress at which fracture occurs is estimated at:

$$\sigma = \sqrt{\frac{8E\mu}{c}} \ . \tag{1}$$

For a brittle medium like glass, μ is the energy of the broken bonds on the fracture surface, but for a ductile medium like a metal, μ is half the much larger energy dissipation by the plastic flow process that takes place at the crack edge during a unit increment of movement. The plastic flow energy dissipation is orders of magnitude larger than the broken-bond surface energy. Hence, metals are much more difficult to fracture than glass or similarly hard, but brittle, materials.

Hard and brittle particles embedded in metals facilitate local fractures in two ways: (1) The particles themselves may fracture to produce a particle-sized crack wide enough to initiate fracture at a low stress, or (2) the presence of the particle in the vicinity of a crack may reduce the energy dissipation required to propagate the crack at least until the crack enlarges to the size of the particle.

A shear stress (τ) acting on the surface of a cylinder of radius (r) and length (L) exerts a maximum tensile force $\tau(2\pi r\, L/2)$ on the cross section, which resists with force $\sigma_{\text{fracture}}\pi r^2$. If the acting tensile stress (σ) is approximately 2τ (maximum shear criterion), then particles fracture if

$$\sigma \geq \frac{2r}{L}\sigma_{\text{fracture}} \ . \tag{2}$$

Other situations, for example, bending moments due to shearing gradients around the FSW pin, require their own particle fracture criteria.

Presumably a crack lying along a rigid, slippery surface would require only about half the plastic energy dissipation that a fully immersed crack would need to propagate. Hence the stress for a slippery, rigid particle to decohere would lower by a factor of $\sqrt{1/2}$ = 0.707 than for propagating a crack in the medium away from the particle.

Where particles fracture or decohere, it may be expected that the resultant particle-sized cracks lower the fracture strength of the medium in accord with the Griffith-Orowan criterion. Hence, the bigger the particle, the lower the strength. Other things being equal, doubling the particle size should reduce the strength by a factor of 0.707.

Large particles in the seam trace of a weld can reduce the strength of the weld appreciably. The fracture surface may be expected to lie along the seam trace, where the big particles are, at least for the fracture initiation site, and large symmetrical ‘tension dimples’ should be visible on the site.

Hence, the need to clean the weld seam surfaces before friction stir welding.

2. TEST PROCEDURE

2.1 Test Objectives

The primary objective of this test program was to compare the effects of laser cleaning to the baseline manual cleaning method on the strength of aluminum panels welded by SR-FSW. Three Nd:YAG pulsed laser cleaning systems from two vendors were evaluated as well as the baseline cleaning method and uncleaned panels as a control.

A secondary objective was to evaluate the effects of cleaning various surfaces of the weld panel to determine the criticality of complete cleaning of the faying surfaces as well as the abutting crown and root surfaces. To use a laser cleaning system on a robotic production weld tool, a complex laser configuration or multiple laser heads would be required to clean all of these surfaces simultaneously.

The test procedure steps were:

(1) Procure and machine three sets of two weld test panels for each cleaning method to be evaluated plus one set of panels to be welded as a control. The cleaning methods to be evaluated were three laser systems with different power levels plus the current manual cleaning method for a total of 24 panels to be cleaned, plus two panels to be welded in the contaminated condition.

(2) Contaminate the test panel surfaces to create a standard contaminant challenge.

(3) Ship or hand deliver the test panels to each cleaning entity, with instructions for the surfaces to be cleaned, standard clean packaging materials, and instructions for packaging and handling of the cleaned panels for return to the MSFC weld lab. Panels cleaned in-house were packaged using the same materials and instructions as those cleaned remotely, and held for a specified period of time to minimize differences in potential recontamination and oxidization from cleaning to welding for the various cleaning methods.

(4) Inspect by scanning electron microscopy (SEM) with energy dispersive x-ray spectroscopy (EDS) a surface cleaned by each method to document initial cleaned condition.

(5) Weld each set of panels, minimizing specimen handling and exposure to an unclean environment before welding.

(6) Section the welded panels perpendicular to the weld and examine the surfaces by metallography.

(7) Machine tensile test specimens from each welded panel and perform tensile tests to assess ultimate yield strength.

2.2 Test Panel Configuration

Standard aluminum test specimens used at MSFC to develop weld schedules and design properties for SR-FSW were used for this experiment. Each weld test specimen consisted of two panels of 2219-T87 aluminum with dimensions of 24 in × 6 in × 0.327 in. For developmental weld tests these panels are abutted and welded along the 24 in length of the 0.327 in surfaces. These panels have a pilot hole drilled centered on the joint near one end to accommodate the SR-FSW tool. The weld panel configuration is shown in figure 1.

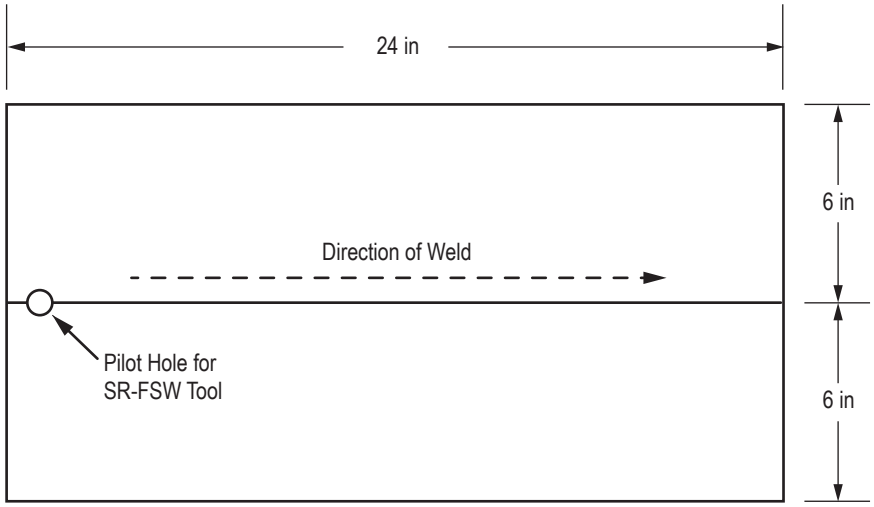

Figure 1. Self-reacting friction stir weld test panel configuration.

After welding, test panels may be examined using nondestructive evaluation methods and then tensile test coupons are machined perpendicular to the weld path and tested to evaluate weld strength.

2.3 Contamination of Test Panels

To assure a consistent contamination challenge, all test panels were anodized to form a surface oxide layer. Surface oxides are known to result in ROD when aluminum is welded by SR-FSW. Anodizing was selected as the contamination method because of the reproducibility of the resulting oxide layer. This is a more severe contamination condition than is typically encountered in production. Usually, weld zones are masked prior to anodizing to prevent the buildup of a hard oxide layer that is difficult to remove prior to welding.

All panels to be cleaned were initially given a 40-minute type II Mil Spec 8625F anodizing treatment and subsequent hot water sealing treatment, which produced an anodized layer thickness of about 7 μ. The type II anodizing treatment is a sulfuric acid treatment (in contrast to type I, a chromic acid treatment, and type III, 'hard anodizing,' a lower temperature sulfuric acid treatment). Type II anodizing leaves a porous surface, but exposure to boiling deionized water

transforms some of the surface coating to an aluminum monohydroxide (boehmite), which reduces surface porosity and seals the surface.

To determine an appropriate anodization time, test samples were anodized for 20, 40, and 60 minutes and sealed. These samples were sectioned and polished, and the anodic coating thicknesses were measured by a microscope at several locations on the surface where the sectioning and polishing had not damaged the anodized surface layer. The results are shown in table 1.

Table 1. Anodized layer thickness for different anodizing times.

Anodizing Time (min)	Anodized Layer Thickness (μ)	Standard Deviation (μ)
20	3.11	0.23
40	7.2	0.33
60	10.48	0.29

The 40-minute anodizing time, resulting in a 7 μ anodized layer thickness, was chosen for preparation of the samples to be cleaned. It was later demonstrated (cleaning set 2) that the 7 μ layer was quite adequate to produce massive residual oxide defect that reduced the strength of the weld coupons to a value too low to be measured unless it was removed from the faying surfaces of the weld seam (cleaning sets 1 and 3).

2.4 Cleaning, Packaging, and Handling of Test Panels

Six anodized test panels were shipped or hand delivered to each cleaning lab to be cleaned by the following equipment:

(1) Lasersystem CL 300Q 300 Watt Nd:YAG, Q-switched, diode pumped laser cleaning unit, Adapt Laser Systems LLC, 1218 Guinotte Ave., Kansas City, MO 64108.

(2) Lasertronics 240 Watt Nd:YAG, Q-switched, diode pumped laser cleaning unit, General Lasertronics Corporation, 830 Jury Court, Suite 5, San Jose, CA 95112.

(3) Backpack Laser CL 20QF-BP, 20 Watt Nd:YAG, adjustable pulsed laser, Adapt Laser Systems LLC, owned and operated by the MSFC Structural Strength Test Branch.

(4) Manual cleaning apparatus of the MSFC Welding and Manufacturing Team.

The three laser teams and the MSFC Welding and Manufacturing team cleaned three sets of two panels. Surfaces on these sets of panels were cleaned as shown in figure 2. On set one,

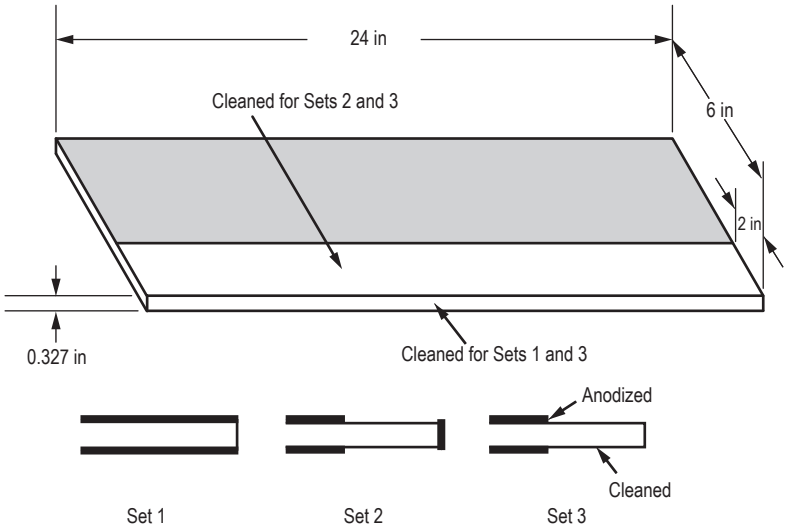

Figure 2. Test panel with surfaces to be cleaned.

only the faying surfaces were cleaned. On set two, only the abutting crown and root surfaces were cleaned. On set three, all of the faying surfaces and abutting crown and root surfaces were cleaned. No surfaces were cleaned on the control panel.

For the panels cleaned manually at MSFC, a draw file was used to clean the faying surfaces in sets 1 and 3 until no oxide was visible. A pneumatic sander with a 3-in-diameter Scotch-Brite™ pad was used to clean the adjacent surfaces for sets 2 and 3.

The laser cleaning labs were instructed to clean the surfaces using laser settings (raster speed, pulse spacing, etc.) of their choosing to provide optimum removal of contaminants and oxides without bulk material damage.

The anodized panels were shipped to the cleaning sites in padded bags. Included were additional bags intended to prevent recontamination and to minimize reoxidation during shipping of the laser cleaned panels back to MSFC. For return shipping, the following packaging procedure was used:

(1) The cleaned panel was placed in Allied Signal (Honeywell) bags of 2-mm-thick Capran® heat-stabilized, nylon-6 film, clean processed.

(2) The nylon bag was purged three times with dry nitrogen and sealed with 2-in, clear packaging tape.

(3) The bagged panel was inserted into a second bag of 6-mm-thick polyethylene, serving as a moisture barrier.

(4) The polyethylene bag was purged three times with dry nitrogen and sealed with 2-in, clear packaging tape.

(5) The packaged panels were placed in padded boxes and shipped overnight so as to arrive at their destination within 24 to 48 hours of the cleaning operation.

Panels that were not shipped but remained at MSFC were bagged just like the shipped panels and held for 24 to 48 hours before processing to minimize differences in handling after cleaning.

2.5 Appearance of Cleaned Surfaces

The objective of this study is to compare the effectiveness of laser cleaning with the effectiveness of manual cleaning.

A manually cleaned surface is shown in figure 3. Tool marks are apparent, indicating the direction of surface abrasion.

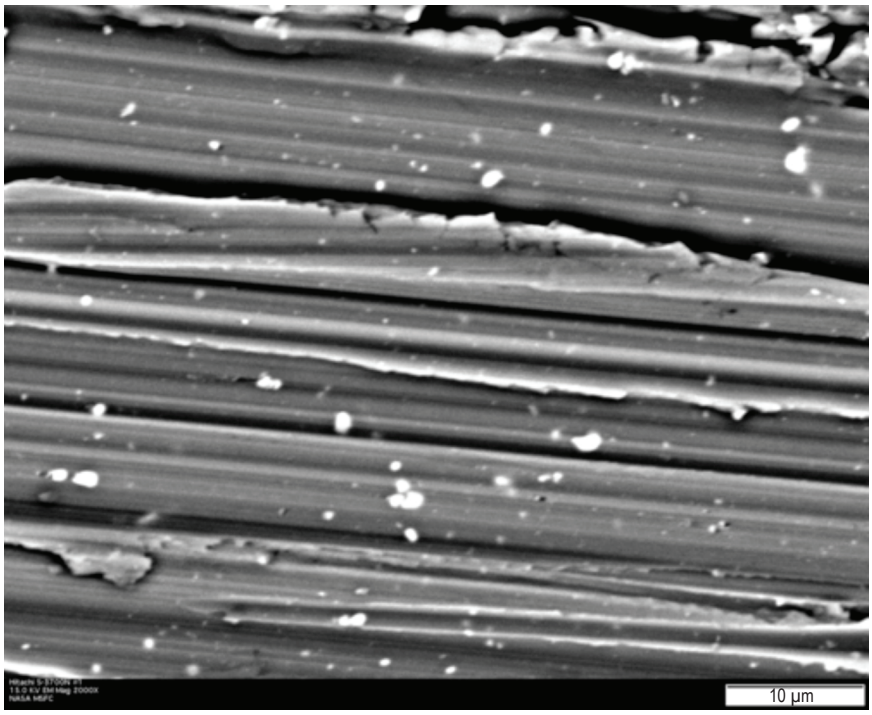

Figue 3. Manually cleaned surface.

Laser cleaned surfaces are shown in figures 4–6. The laser cleaned surfaces are characterized by flow of molten material beam strike craters. Electron Dispersion Spectroscopy, carried out in conjunction with SEM used to observe the laser cleaned surfaces, revealed sulfur contamination of the surfaces, presumably due to the exposure to sulfuric acid during the anodization process. The laser cleaned surfaces all exhibit flow of molten material around beam strike craters and a dark contrast material that increases in area as the power of the laser diminishes.

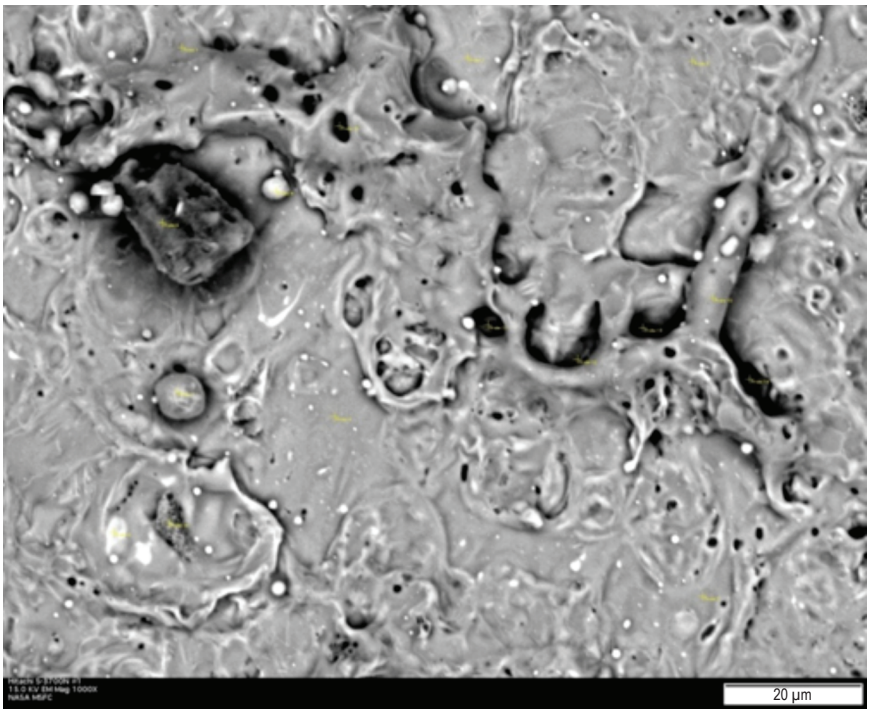

Figure 4. Laser cleaned surface (300 W, Adapt Laser Systems).

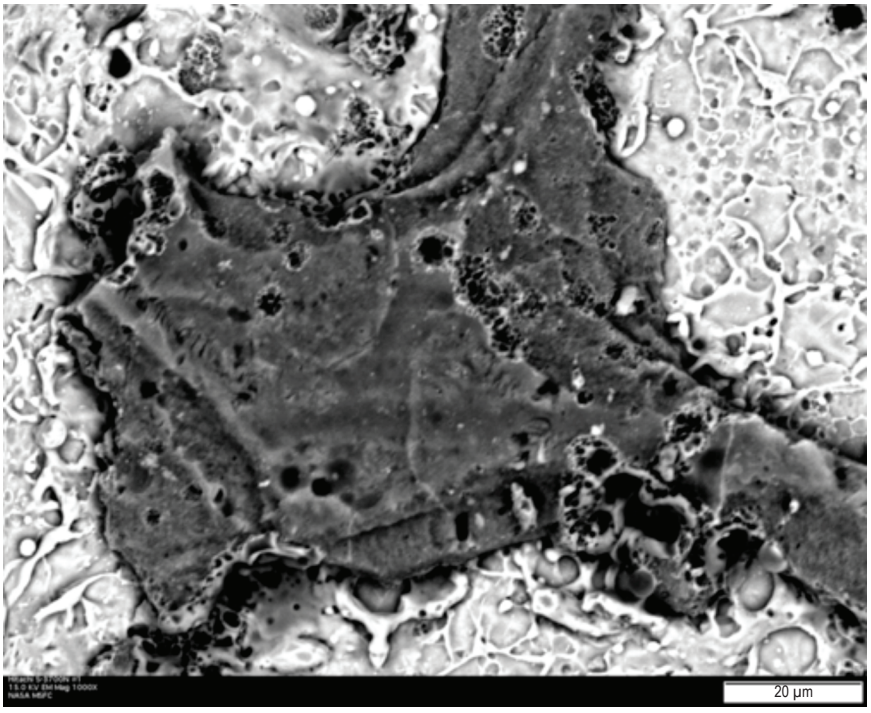

Figure 5. Laser cleaned surface (240 W, General Lasertronics Corp.).

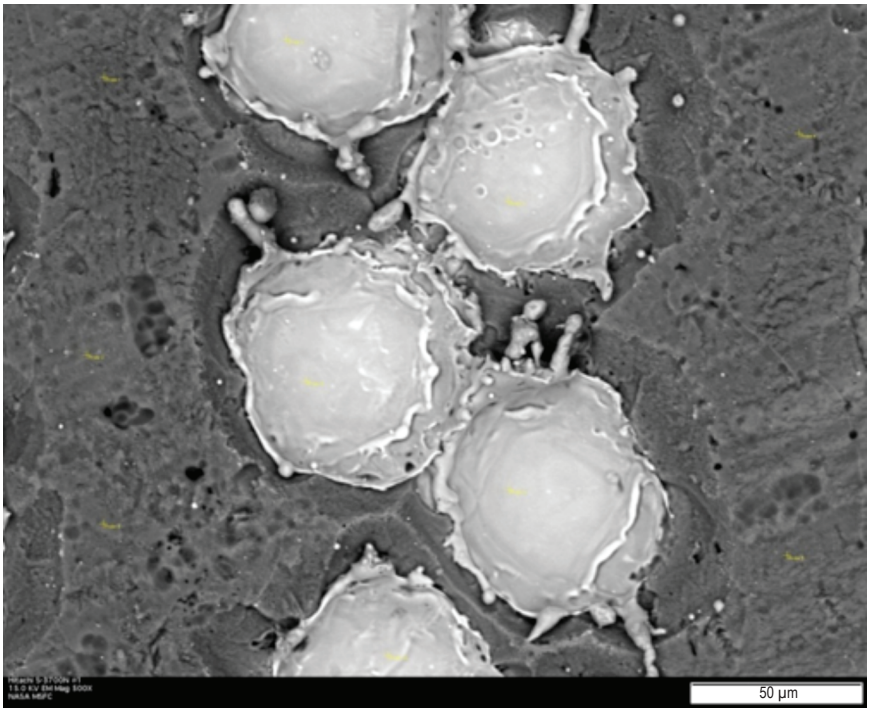

Figure 6. Laser cleaned surface (20 W, Adapt Laser at MSFC).

The strike crater overlap and intensity of laser cleaning can be adjusted by modification of the laser wattage, pulse frequency, travel speed, and other factors. The laser strike craters in figure 6 do not overlap, indicating that the settings on the 20 W laser may have been insufficient to remove surface oxide contamination. A more extensive analysis of the effects of laser wattage, pulse frequency, travel speed, pulse crater overlap, and other control settings on oxide removal and weld strength would require a large test matrix. Such analysis is beyond the scope of this preliminary evaluation.

A similar pair of panels was prepared and left uncleaned for a weld control sample. An uncleaned control surface is shown in figure 7.

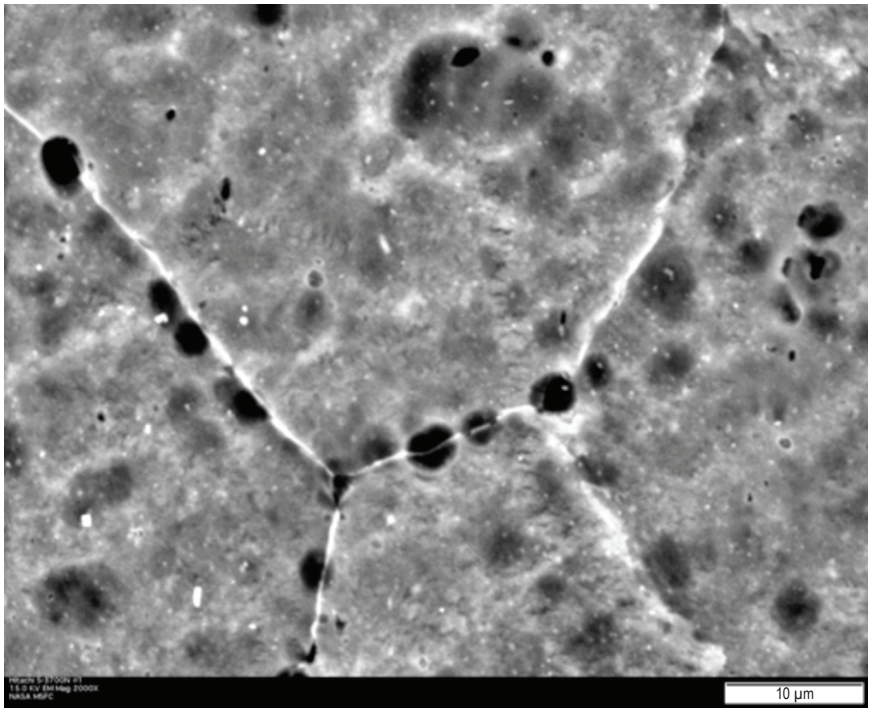

Figure 7. Uncleaned control surface.

2.6 Welding

At MSFC, the returned and resident panels having been cleaned according to the prescriptions of sets 1–3 were paired for welding: 3 manually cleaned welds, 9 laser cleaned welds, and 1 uncleaned control, for a total of 13 welds.

The weld operators were instructed to handle the precleaned panels with clean gloves and to omit standard precleaning procedures. A starting hole for the SR-FSW tool was drilled through the center of the weld (no offset) at the beginning of the weld seam. Each weld panel was clamped in Horizontal Weld Tool #30A-72251 located in Building 4755 and welded with a Boeing Tri-Flat SR-FSW tool shown in figure 8. The panels were welded using nominal weld parameters of spindle speed, travel speed, and load, optimized for 0.327-in 2219 weld joints. A typical welded panel is shown in figure 9.

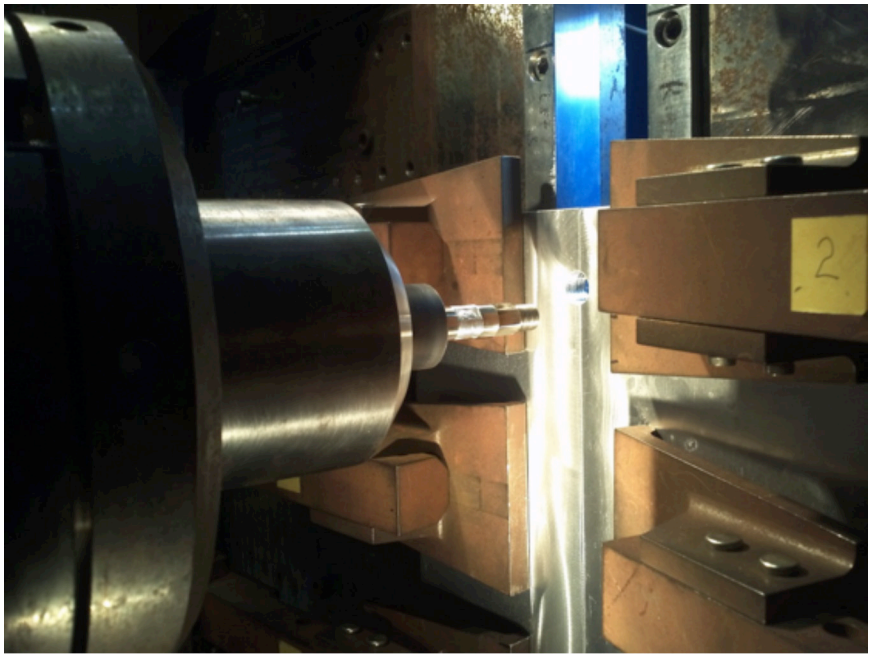

Figure 8. Horizontal FSW panel setup.

Figure 9. Self-reacting friction stir welded panel.

3. ANALYSIS AND RESULTS

3.1 Analysis Procedures

Each welded panel was sectioned perpendicular to the weld for metallography and to create tensile specimens to test the strength of each weld.

Metallography specimens were prepared by cutting, mounting, polishing, and etching transverse sections of the welded zones. These specimens were evaluated and photographed under magnification for evidence of ROD.

Five tensile coupons each were machined from 11 of the 13 welded panels. Two of the panels yielded such low bond strength that machining of tensile coupons was not feasible. The tensile coupon configuration was a rectangular bar, perpendicular to the weld path, with a nominal cross-sectional area of 0.33 in^2.

Tensile testing was conducted in accordance with MSFC Mechanical Test Lab standard work instructions, on test station 8 in MSFC Building 4602. The environment for this testing was ambient laboratory air. The mechanical test frame consisted of a servo-hydraulic actuator and reaction frame. A 60,000-lb load cell and 25-in cable extension transducer were installed on the frame. An extensometer with a 2-in-gauge length and 50% range was installed on each specimen prior to testing. Each specimen was preloaded to 100 lb and then ramped to failure at a rate of 0.05 in/min. One inch and two inch punch marks were used to indicate elongation around the weld zone. Stress-strain curves were plotted for each tensile test and data were recorded for tensile stress (ksi), yield stress (ksi), inelastic strain (%), modulus of elasticity (msi), and fracture elongation (%).

3.2 Visual Results for the Baseline Method—Manual Cleaning

The transverse sections of the welded manually cleaned surfaces (fig. 10) exhibited tool marks but no apparent ROD. The welds exhibited the banding characteristic of friction stir welds with the reticulated structure characteristically imposed by flats on the tool and a hint of the onion-ring structure characteristic of threaded tools without flats.

Figure 10. Transverse section of manually cleaned weld.

The fracture surface of the tensile test specimens (fig. 11) is angular, i.e., a ductile fracture. Angular fractures result from shear. The plane of maximum shear at 45º to the direction of applied tensile stress is favored for shear, although hardness variation within the weld may make shear easier on a plane at a somewhat different angle. Fracture occurs when tiny pores elongate with strain and combine to a point where the residual fracture surface area supports less and less shear stress, or sooner if defects or dirt within the weld metal promotes local ruptures.

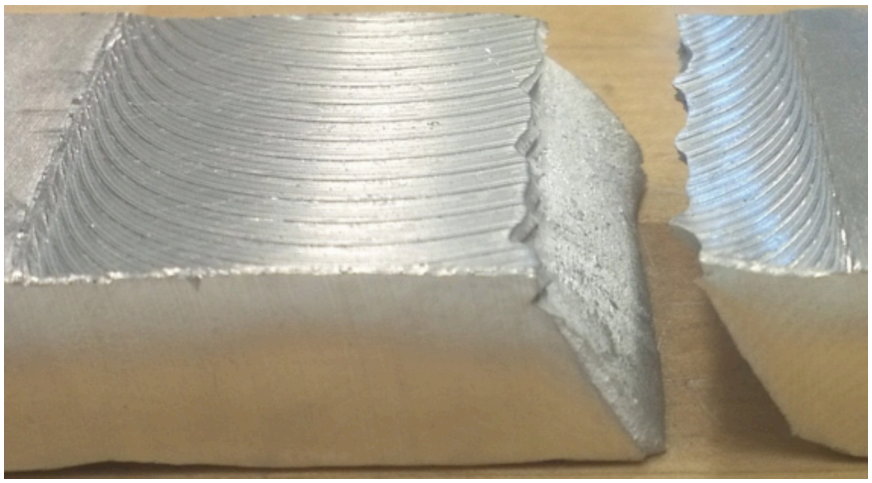

Figure 11. Fracture surface of manually cleaned weld. Note angular ductile fracture.

3.3 Visual Results for the Worst Case Method—No Cleaning

The uncleaned anodized surface, shown in figure 7, is covered with a layer of aluminum oxide about 7 μ thick. Dark spots, possibly carbon, tending to line up along grain boundaries, are present. Sulfur from the anodizing process is also detectable by EDS.

The transverse sections of welded uncleaned surfaces, shown in figure 12, exhibited a fine, sharp, slightly undulating white line running from root to crown close to the center of the weld. This is indicative of ROD, where the oxide particles remain in place along the seam and serve to mark its location on the weld transverse section. When a weld seam increment is 'wiped' onto the rotating plug of metal attached to the friction stir tool, a powerful shearing action expands the seam area along the plug surface, cracks the oxide, and presents clean metal surface, which is compressed into contact so that it bonds. The seam is recompressed by a countershear process when the tool abandons it in its wake.

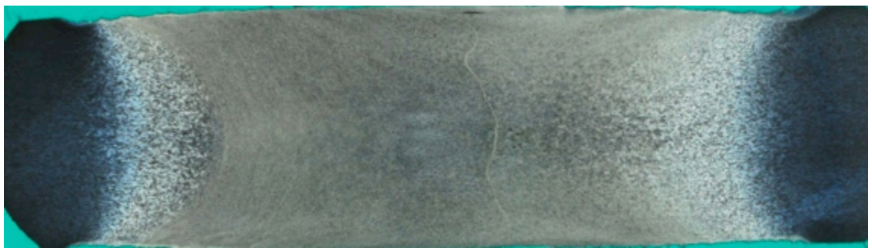

Figure 12. Transverse section of uncleaned weld. Note the fine, sharp, slightly undulating white line running from root to crown, close to the center of the weld indicating ROD.

The perpendicular, slightly undulating fracture surface of the tensile specimen (fig. 13) follows the seam trace seen in figure 12, now made susceptible to propagation of fissures perpendicular to the direction of tensile stress by the residual oxide, with the characteristic of a brittle fracture. This correlates with extremely low fracture strength of the uncleaned welds.

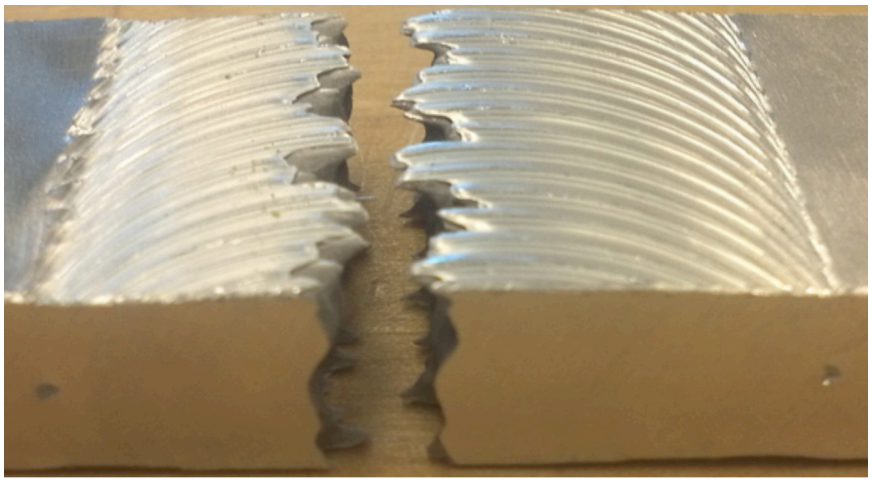

Figure 13. Fracture surface of uncleaned weld. Note perpendicular nonductile fracture with undulations resembling those of the white line shown in figure 12.

This seam trace is characteristic of a weld tool with flats. The threads (or shoulder scrolls) on the tool drive a relatively slow ring vortex circulation around the tool, while tool eccentricity or flats induce a more rapid pumping of metal in and out from the tool. The ring vortex circulation through an inward radial flow component at the tool shoulders keeps metal inside the rotating plug longer and shifts streamlines (and tracers) toward the advancing side of the tool. The corresponding outward radial flow component at the pin center expels streamlines sooner from the rotating plug and shifts them toward the retreating side of the tool. By itself the ring vortex circulation transforms the straight vertical trace of the seam entering the rotating plug to a broad loop extending from the advancing side of the rotating plug at the crown and root surfaces to the retreating side of the plug at the weld center.[1]

Flats on a tool appear to reduce the distortion of the seam trace in transverse section, presumably by reducing the amount of thread driving the ring vortex motion.[2] Hence, the seam trace with its ROD, while not straight, is more vertical and a closer approximation to a section of the original seam than would be the case with a tool without flats.

Tool eccentricity pumping drives the metal back and forth in the softened regions at the shear surface bounding the rotating plug so as to generate textural variations with a periodicity of the tool rotation. The texture variations give rise to etching contrast and are responsible for the internal banding seen in transverse weld section as onion rings. It is also responsible for the formation of surface ripples called 'tool marks.'

Study of the effect of flats and tool geometry in general is currently under way.[2] At circumferential locations on the tool where the radius about the center of rotation increases, it is anticipated that metal flows out, pumped away from the tool, and at locations where the radius decreases, metal is drawn in. Each flat adds a periodic perturbation to the effect of the eccentricity of the tool. The perturbation effect is complicated, however, by at least two effects:

(1) As the perturbation circumferential distances shorten with numbers of flats and as the metal softens with higher temperatures, it becomes easier for circumferential flow to compete with radial flow. It is anticipated that the effect should diminish with increasing numbers of flats and higher tool revolutions per minute.

(2) The phase relation between the flats and the tool eccentricity is anticipated to affect the details of the structural effect from tool to tool. The reticulated band patterns and the flattening and the undulations in the trace of the weld seam associated with flats are thought to be due to this perturbation.

3.4 Visual Results for Laser Cleaning

The transverse sections of the welded panels that were cleaned by laser (figs. 14–16) all exhibit the fine, sharp, slightly undulating white line of the ROD running from root to crown, close to the center of the weld. These lines are less distinct than seen in the weld of the uncleaned surfaces, and at the higher laser powers, seem to disappear intermittently.

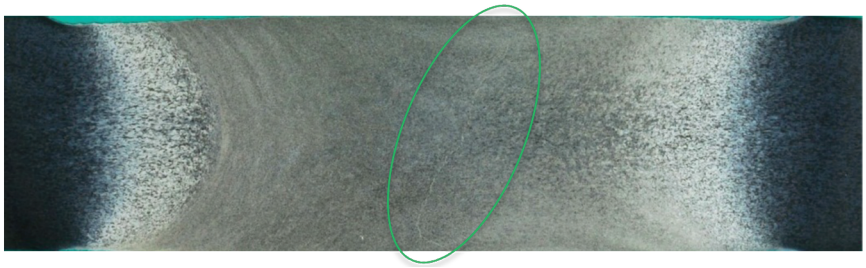

Figure 14. Transverse section of laser cleaned weld (300 W, Adapt Laser Systems). Note the fine, sharp, slightly undulating white line running from root to crown toward the center of the weld indicating ROD.

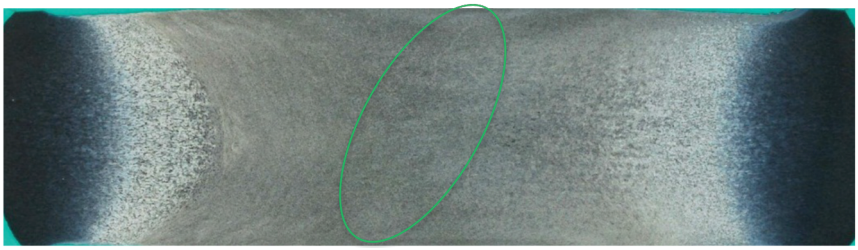

Figure 15. Transverse section of laser cleaned weld (240 W, General Lasertronics). Note the fine, sharp, slightly undulating white line running from root to crown toward the center of the weld indicating ROD.

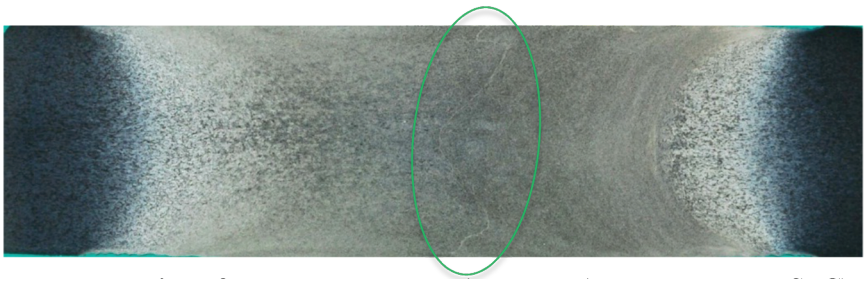

Figure 16. Transverse section of laser cleaned weld (20 W, Adapt Laser at MSFC). Note the fine, sharp, slightly undulating white line running from root to crown toward the center of the weld indicating ROD.

The tensile specimens from the welded laser cleaned panels all exhibit perpendicular, slightly undulating fracture surfaces (figs. 17–19), appearing to follow the seam trace and signifying nonductile fractures.

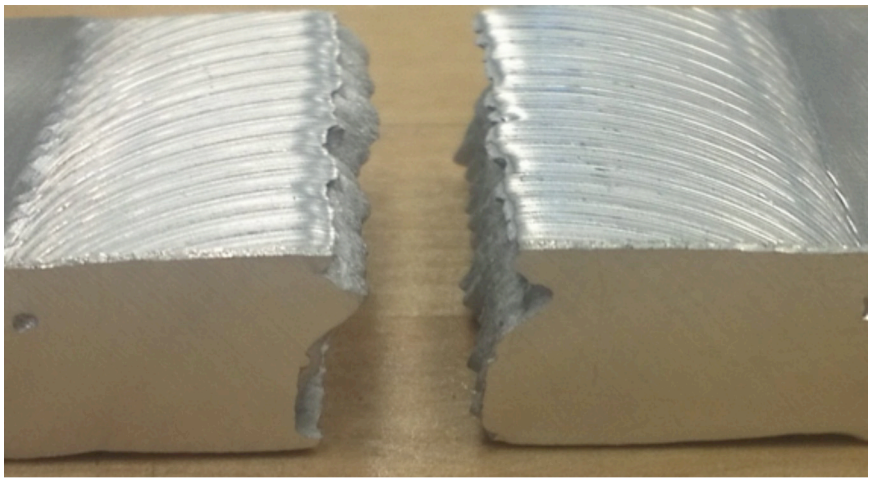

Figure 17. Fracture surface of laser cleaned weld (300 W, Adapt Laser Systems). Note perpendicular nonductile fracture.

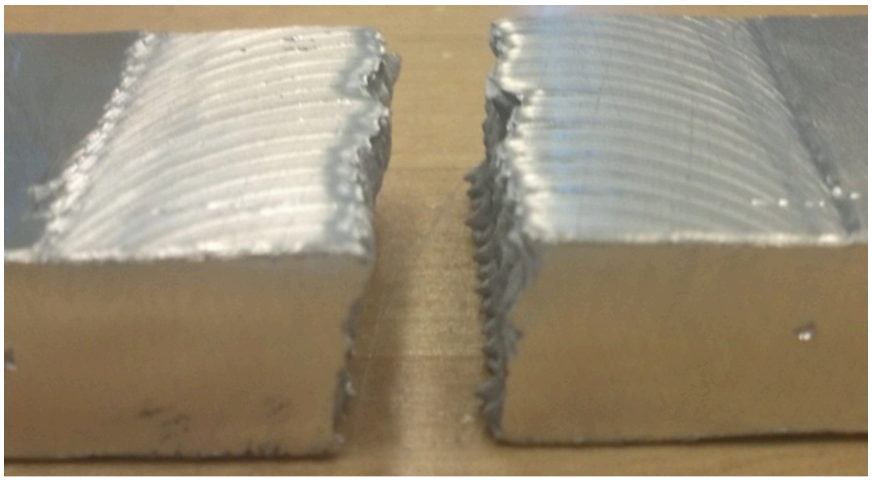

Figure 18. Fracture surface of laser cleaned weld (240 W, General Lasertronics). Note perpendicular nonductile fracture.

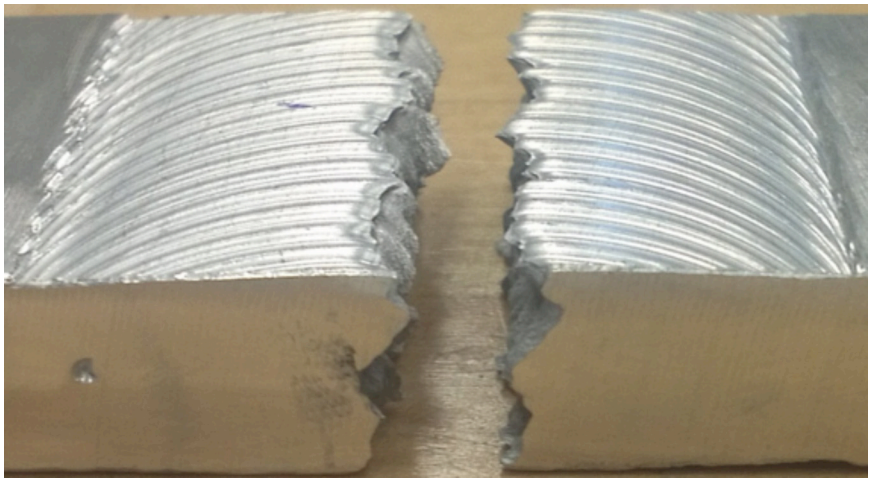

Figure 19. Fracture surface of laser cleaned weld (20 W, Adapt Laser at MSFC). Note perpendicular nonductile fracture.

3.5 Tensile Test Results

Tensile test results for the welded panels subjected to the various cleaning methods are shown in table 2. This table displays average ultimate tensile strength and standard deviation of five coupons cut from each of the welds. Excessively low tensile strengths could not be measured for two of the five coupons from the uncleaned weld. No tensile data could be obtained for two of the three laser cleaned welds where the faying surfaces had not been cleaned. Tensile test coupons could not be produced because these welds failed to adequately bond. These results are displayed graphically in figure 20.

Table 2. Ultimate tensile strength of welds subjected to various cleaning methods.

Cleaning Method	Cleaning Coverage	Average Ultimate Tensile Strength (ksi)	Standard Deviation (ksi)
Baseline—Manual cleaning at MSFC	Faying surface only	43.16	4.48
	Adjacent crown and root surfaces, but not faying surface	NA*	NA*
	Faying surface plus adjacent crown and root surfaces	46.84	1.35
300 W laser at Adapt Laser Systems	Faying surface only	35.77	4.82
	Adjacent crown and root surfaces, but not faying surface	NA*	NA*
	Faying surface plus adjacent crown and root surfaces	29.16	5.22
240 W laser at General Lasertronics Corporation	Faying surface only	27.10	0.91
	Adjacent crown and root surfaces, but not faying surface	19.08	1.67
	Faying surface plus adjacent crown and root surfaces	28.19	0.18
20 W Adapt Laser System at MSFC	Faying surface only	27.58	1.98
	Adjacent crown and root surfaces, but not faying surface	14.21	4.42
	Faying surface plus adjacent crown and root surfaces	24.81	2.63
Control	No surfaces cleaned	2.4**	2.8**

*No tensile data were obtained from these test sets. The welds failed to bond adequately to machine tensile test coupons.

**Average ultimate tensile strength and standard deviation of three tests. In this test set, two of the five tensile tests failed at a level too low to measure.

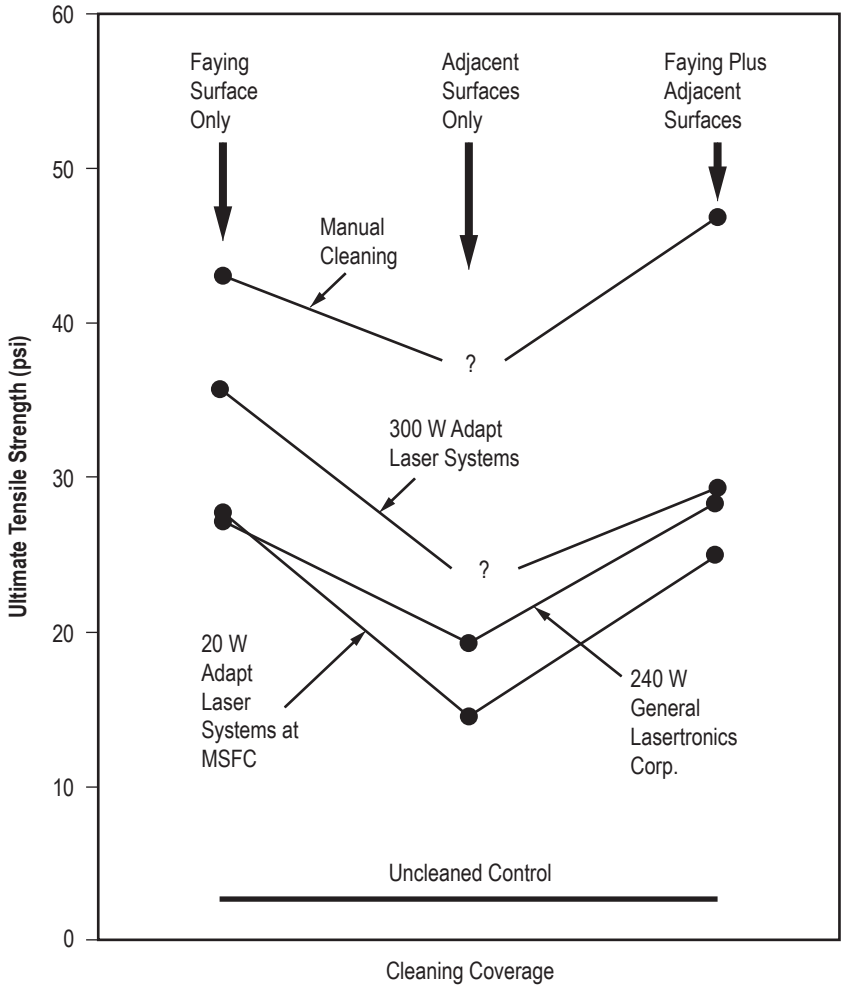

Figure 20. Weld strengths as they vary with cleaning method and coverage.

Average tensile strengths of the laser cleaned welds all measured substantially below that of the manually cleaned surface welds and substantially above that of the uncleaned surface weld. It was clear from the results for the uncleaned weld that surface oxide contamination is devastating to weld strength. Higher laser powers roughly correlated with stronger welds.

From the tensile strength results it is clear that the faying surface is the critical surface that must be cleaned. Cleaning the adjacent crown and root surfaces of the manually cleaned panels in addition to the faying surfaces increased the weld strength by 8.5%. The effect of cleaning the adjacent surfaces on the laser cleaned panels was inconsistent, varying from 4% to –18.5%. Surface contamination from the adjacent surfaces may be ingested into the body of the weld, swept in by the ring vortex circulation. It is possible that surface anodization could interfere with internal flow processes by blocking tool mark surface ripples. The reason for the varied strength effect of adjacent surface cleaning is unclear.

4. CONCLUSIONS

Only the current manual cleaning practice appeared to remove oxide well enough to eliminate ROD. All of the attempts to laser clean the anodized 2219 aluminum alloy test samples left sufficient residual oxide on the weld seam surface to substantially reduce the strength of a friction stir weld. Laser cleaning, where at least the faying surface was cleaned, yielded weld strengths that were superior to no cleaning but insufficient to consider the laser cleaning as a potential replacement for manual cleaning at this time.

This does not mean that lasers cannot remove ROD from anodized aluminum alloys adequately for welding surface preparation, but it implies that a more sophisticated approach to the task than cut-and-try is required. The more sophisticated approach would presumably entail physical modeling of the process underlying ROD removal and a more extensive test matrix to evaluate the effects of specific laser cleaning process variables.

It may also be questioned whether the test to remove the oxide layer from anodized aluminum is more stringent than required for removal of normal surface contamination prior to FSW. Typically, aluminum is not anodized prior to welding. When parts are to be anodized prior to welding, the planned weld zones are masked to prevent oxide build up. Also, it is possible that residual sulfur from the anodization process may affect weld quality more than other forms of naturally occurring oxide. However, designing a test to remove naturally occurring contamination and oxides can be difficult because these may be highly variable. A study would be required to determine what constitutes normal surface contamination. ROD is encountered now and then in the real world of welding. It may be that some naturally occurring variations of surface contamination are particularly difficult to remove or easy to overlook.

A secondary conclusion from this study is that it is essential to clean the faying surfaces of the weld seam. It is not nearly as critical to clean the adjacent crown and root surfaces, and in the case of laser cleaning, could either raise or lower the resulting weld strength.

In addition, it was observed that residual oxide on the weld seam surface serves as a tracer, yielding information about the effect of the flats on the Boeing Tri-Flat tool used to make the weld. The flats appear to perturb the looped structure of the seam trace on the weld transverse section into a flatter, undulating trace. Weld tensile test fractures appear to follow this trace with corresponding undulations.

5. RECOMMENDATIONS FOR FUTURE STUDY

Although the performance of laser cleaning prior to FSW was inferior to the current manual cleaning process in this preliminary study, the potential for savings in time and touch labor costs may justify further investigation of laser cleaning processes. Weld specimens cleaned by laser methods did show improvements over no cleaning and it is unclear whether improved laser process parameters on naturally occurring contaminants and oxides could achieve weld strengths comparable to manual cleaning.

The following changes to this test design are recommended for further study of laser cleaning as an alternative surface preparation method for friction stir welding:

(1) Prepare contaminated test panels by methods other than sulfuric acid anodizing. Contaminants could include naturally occurring oxides from random production pieces, contaminants on cut panels left to oxidize under controlled conditions, or a less aggressive form of induced oxidation such as conversion coating.

(2) Design a more extensive test matrix to evaluate the effects of laser cleaning process variables on weld strength and potentially determine whether these variables could be tailored to achieve weld strength comparable to that achieved with manual cleaning. Laser cleaning variables may include laser wattage, dwell time, spot overlap (controlled by travel speed and raster spacing), or other parameters recommended by the laser manufacturers.

(3) Include cleaning of the panel faying surfaces in all test scenarios. Scenarios may include laser cleaning of all test surfaces or laser cleaning of the crown and root surfaces combined with manual cleaning of the faying surfaces.

Given the resources for a comprehensive study, in order to assess the ultimate capability of the laser for removal of various kinds of surface contamination and to assist in determination of optimal parameters, it is recommended that a study of the mechanism of laser cleaning be carried out.

Once the ultimate capability of the laser for removal of various kinds of surface contamination is established, a survey of actual preweld surface contamination would allow an assessment of the capability of the laser for surface preparation of friction stir welds.

REFERENCES

1. Rubisoff, H.A.; Schneider, J.A.; and Nunes, Jr., A.C.: "Control of Structure in Conventional Friction Stir Welds through a Kinematic Theory of Metal Flow," *Friction Stir Welding and Processing-V*, The Minerals, Metals & Materials Society, pp. 149–158, 2009.

2. Boves, E.: "Pin Tool Analysis Using Conventional Friction Stir Welding (FSW)," Unpublished Report: NASA Summer Student Project, Marshall Space Flight Center, 2012.

REPORT DOCUMENTATION PAGE

Form Approved
OMB No. 0704-0188

1. REPORT DATE *(DD-MM-YYYY)*	2. REPORT TYPE	3. DATES COVERED *(From - To)*
01–02–2014	Technical Memorandum	

4. TITLE AND SUBTITLE

Laser Ablation Cleaning of Self-Reacting Friction Stir Weld Seam Surfaces: A Prelimiary Evaluation

5a. CONTRACT NUMBER

5b. GRANT NUMBER

5c. PROGRAM ELEMENT NUMBER

6. AUTHOR(S)

A.C. Nunes, Jr., C.K Russell, S.A Brooke, Q. Parry,*
and N.M. Lowrey**

5d. PROJECT NUMBER

5e. TASK NUMBER

5f. WORK UNIT NUMBER

7. PERFORMING ORGANIZATION NAME(S) AND ADDRESS(ES)

George C. Marshall Space Flight Center
Huntsville, AL 35812

8. PERFORMING ORGANIZATION REPORT NUMBER

M–1376

9. SPONSORING/MONITORING AGENCY NAME(S) AND ADDRESS(ES)

National Aeronautics and Space Administration
Washington, DC 20546–0001

10. SPONSORING/MONITOR'S ACRONYM(S)

NASA

11. SPONSORING/MONITORING REPORT NUMBER

NASA/TM—2014–217500

12. DISTRIBUTION/AVAILABILITY STATEMENT

Unclassified-Unlimited
Subject Category 31
Availability: NASA STI Information Desk (757–864–9658)

13. SUPPLEMENTARY NOTES

Prepared by the Materials & Processes Laboratory, Engineering Directorate
*University of Utah, Salt Lake City, UT **Jacobs ESSSA Group, Huntsville, AL

14. ABSTRACT

Anodized aluminum panels were cleaned by three lasers at three separate sites with a view to determining whether more economical laser cleaning might supplant current manual cleaning methods for preparation of surfaces to be welded by the self-reacting friction stir process. Uncleaned panels yielded welds exhibiting residual oxide defect (ROD) and failing at very low stresses along the trace of the weld seam. Manually cleaned panels yielded welds without ROD; these welds failed at nominal stress levels along an angled fracture surface not following the weld seam trace. Laser cleaned panels yielded welds failing at intermediate stress levels. The inadequacy of the laser cleaning processes leaves questions: Was the anodized aluminum test too stringent to represent actual cleaning requirements? Were the wrong laser cleaning techniques/parameters used for the study? Is the laser cleaning mechanism inadequate for effective preweld surface cleaning?

15. SUBJECT TERMS

friction stir welding, weld preparation, laser cleaning, residual oxide defect

16. SECURITY CLASSIFICATION OF:			17. LIMITATION OF ABSTRACT	18. NUMBER OF PAGES	19a. NAME OF RESPONSIBLE PERSON
a. REPORT	b. ABSTRACT	c. THIS PAGE			STI Help Desk at email: help@sti.nasa.gov
U	U	U	UU	40	19b. TELEPHONE NUMBER *(Include area code)* STI Help Desk at: 757–864–9658

National Aeronautics and
Space Administration
IS20
George C. Marshall Space Flight Center
Huntsville, Alabama 35812